

Lattice solitons in \mathcal{PT} -symmetric mixed linear-nonlinear optical lattices

Yingji He,^{1,*} Xing Zhu,² Dumitru Mihalache,³ Jinglin Liu,¹ and Zhanxu Chen¹

¹*School of Electronics and Information, Guangdong Polytechnic Normal University, 510665 Guangzhou, China*

²*State Key Laboratory of Optoelectronic Materials and Technologies, Sun Yat-Sen University, 510275 Guangzhou, China*

³*Horia Hulubei National Institute for Physics and Nuclear Engineering, P.O. Box MG-6, RO-077125 Magurele-Bucharest, Romania*

(Received 17 December 2011; published 23 January 2012)

We report the existence and stability of lattice solitons in parity-time (\mathcal{PT})-symmetric mixed linear-nonlinear optical lattices in Kerr media. We focus on studying the characteristic effects on soliton propagation in the semi-infinite gap if we consider different amplitudes of real and imaginary parts of both the linear refractive index modulation profile and of periodic nonlinearity-modulation spatial distribution. It was found that the combination of \mathcal{PT} -symmetric linear and nonlinear lattices can stabilize lattice solitons and can provide unique soliton properties. It is revealed that the parameters of the linear lattice periodic potential play a significant role in controlling the extent of the stability domains and that the lattice solitons can stably propagate only in the low-power regime.

DOI: [10.1103/PhysRevA.85.013831](https://doi.org/10.1103/PhysRevA.85.013831)

PACS number(s): 42.65.Tg, 42.65.Sf

I. INTRODUCTION

Since 1998, after the publication of the seminal work of Bender and Boettcher [1], who introduced the concept of parity-time (\mathcal{PT})-symmetric complex-valued potentials, there has been a lot activity in this area due to emerging applications in various physical settings, especially in the field of optics and photonics. In their pioneering work, Bender and Boettcher found that non-Hermitian Hamiltonians can still have entirely real eigenvalue spectra provided that these Hamiltonians respect \mathcal{PT} symmetry. Moreover, it was demonstrated that such types of Hamiltonians can also undergo a phase transition above a critical threshold, i.e., a spontaneous \mathcal{PT} symmetry breaking; above such transition point the eigenvalue spectrum ceases being entirely real and becomes partially complex [2–5]. Thus, for a general Hamiltonian $\hat{H} = \hat{p}^2/2 + V(\hat{x})$, where \hat{p} and \hat{x} are the momentum and position operators, respectively, one can deduce that a necessary condition (but not a sufficient one) for the Hamiltonian to be \mathcal{PT} symmetric is that the potential function $V(x)$ should fulfill the condition $V(x) = V^*(-x)$ [1,6–8]. In other words, the real part of the \mathcal{PT} complex potential must be an even function of the position x , whereas the imaginary part should be an odd function of the variable x . The \mathcal{PT} -symmetric potentials can be realized through using the complex refractive index distribution $n(x) = n_0 + n_R(x) + in_I(x)$, where n_0 represents the background refractive index and x is the normalized transverse coordinate [6,7]. To satisfy the \mathcal{PT} symmetry condition, $n_R(x)$ must be an even function of the transverse spatial coordinate x , while the gain or loss component $n_I(x)$ should be an odd one.

Passive \mathcal{PT} symmetry breaking within the realm of optics was demonstrated experimentally by Guo *et al.* [9]. This first observation of such \mathcal{PT} symmetry breaking in complex-valued optical potentials means that the corresponding phase transition leads to a loss-induced optical transparency in specially designed pseudo-Hermitian guiding optical potentials. Later, Rüter *et al.* [10] reported the observation of both

spontaneous \mathcal{PT} symmetry breaking and power oscillations violating left-right symmetry. In the theoretical arena, the early incentive work of Musslimani *et al.* [6] studied the effect of Kerr nonlinearity on the unique beam dynamics in \mathcal{PT} -symmetric complex-valued periodic optical potentials, i.e., the formation of nonlinear self-trapped modes, alias optical solitons in both one-dimensional (1D) and two-dimensional (2D) \mathcal{PT} -symmetric synthetic linear optical lattices (OLs). The study of \mathcal{PT} -symmetric linear OLs [7,8,11], has also attracted much attention during the past few years. Beam dynamics in \mathcal{PT} -symmetric complex-valued periodic lattices can exhibit unique characteristics, such as double refraction, power oscillations, nonreciprocal diffraction patterns, etc. [7]. Defect modes in \mathcal{PT} -symmetric periodic complex-valued potentials have also been studied [12,13]. Recently, we studied gap solitons in parity-time complex-valued periodic OLs with the real part of the linear lattice potential having the shape of a double-periodic function (a superlattice potential) [14]. Stable 1D and 2D bright spatial solitons in defocusing Kerr media with \mathcal{PT} -symmetric potentials have also been found [15]. Bragg gap solitons in \mathcal{PT} -symmetric lattices with competing optical nonlinearities of the cubic-quintic type have been also investigated in a recent study [16].

Of much interest from both a theoretical and experimental point of view is the study of solitons in *nonlinear optical lattices*; see a recent comprehensive review in this area [17]. Such nonlinear OLs represent a spatially periodic modulation of the local strength and sign of the optical nonlinearity. It should be mentioned that \mathcal{PT} -symmetric nonlinear OLs can also support stable discrete solitons [18]; for a comprehensive review of discrete solitons in optics, see Ref. [19]. We also bring readers' attention to a series of recent incentive works in the area of \mathcal{PT} -symmetric nonlinear lattices in various physical settings [20–22]. The existence of localized modes, including multipole solitons, supported by \mathcal{PT} -symmetric nonlinear lattices was recently reported [20]. Such \mathcal{PT} -symmetric nonlinear OLs can be implemented by means of proper periodic modulation of nonlinear gain and losses, in specially realized nonlinear optical waveguides. It was found in Ref. [20] that unlike other typical dissipative systems, stable one-parameter families of localized solutions do exist

*heyinji8@126.com

even when the conservative part (i.e., the real part) of the complex-valued nonlinear periodic potential is absent.

Solitons in periodic mixed lattices with linear and nonlinear counterparts have also been investigated. To the best of our knowledge, the issue of competition between the lattices of the linear and nonlinear types was first investigated by Bludov and Konotop [23] in the context of matter waves in Bose-Einstein condensates (BECs); see also a subsequent work [24] on gap solitons in BECs loaded in mixed linear-nonlinear optical lattices. However, to the best of our knowledge, solitons in \mathcal{PT} -symmetric mixed linear-nonlinear optical lattices have not been studied yet.

In this work, we perform a comprehensive study of the existence and stability of lattice solitons in Kerr media, which are confined by \mathcal{PT} -symmetric complex-valued periodic potentials, representing the superposition of linear and nonlinear optical lattices. Thus we consider a mixture of a linear lattice (grating) and a nonlinear lattice (i.e., a periodic transverse modulation of both cubic nonlinearity and nonlinear gain). We vary the amplitudes of real and imaginary parts of linear refractive index modulation profile (i.e., the relevant parameters of the linear lattice profile) and the corresponding amplitudes of the complex-valued periodic nonlinearity-modulation profile (i.e., the relevant parameters of the nonlinear lattice profile). It was found that the jointly acting \mathcal{PT} -symmetric linear and nonlinear periodic potentials can stabilize lattice solitons and can provide unique soliton properties. It is revealed that the parameters of the linear lattice periodic potential play a significant role in controlling the magnitude of the stability domain and that the lattice solitons can stably propagate only for low powers; i.e., the solitons with powers larger than some threshold values are linearly unstable.

II. THE GOVERNING MODEL

Beam propagation in the \mathcal{PT} -symmetric mixed linear-nonlinear OLs with focusing Kerr nonlinearity obeys the following normalized 1D nonlinear Schrödinger equation [6]:

$$i \frac{\partial q}{\partial z} + \frac{1}{2} \frac{\partial^2 q}{\partial x^2} + [v(x) + iw(x)]q + |q|^2 q + [v_1(x) + iw_1(x)]|q|^2 q = 0, \quad (1)$$

where q is the complex field amplitude and z is the normalized longitudinal coordinate. We search for stationary solutions of Eq. (1) in the form $q = f(x) \exp(i\mu z)$, where $f(x)$ is a complex-valued function, and μ is the corresponding real propagation constant. In such case, the complex function $f(x)$ satisfies the following differential equation:

$$\frac{1}{2} \frac{d^2 f}{dx^2} + [v(x) + iw(x)]f + |f|^2 f + [v_1(x) + iw_1(x)]|f|^2 f = \mu f. \quad (2)$$

By substituting $f(x) = h(x) + ie(x)$ into Eq. (2), we obtain the two coupled equations:

$$\begin{aligned} \frac{1}{2} h_{xx} + vh - we + h^3 + he^2 + v_1 h^4 - 2w_1 h^3 e - 2w_1 h e^3 - v_1 e^4 &= \mu h, \end{aligned} \quad (3a)$$

$$\begin{aligned} \frac{1}{2} e_{xx} + ve + wh + h^2 e + e^3 + w_1 h^4 + 2v_1 h^3 e + 2v_1 h e^3 - w_1 e^4 &= \mu e, \end{aligned} \quad (3b)$$

where h and e are real functions.

The linear version of Eq. (2) is

$$\frac{1}{2} \frac{d^2 f}{dx^2} + [v(x) + iw(x)]f = \mu f. \quad (4)$$

The Bloch theorem tells us that the eigenfunctions of Eq. (4) are of the form $f = F_k \exp(ikx)$, where k is the Bloch wave number, and F_k is a periodic function of x with the same period as the linear lattice profiles $v(x)$ and $w(x)$. Substituting the Bloch solution into Eq. (4), we get the eigenvalue equation

$$\left(\frac{d^2}{dx^2} + 2ik \frac{d}{dx} - k^2 \right) F_k + [v(x) + iw(x)]F_k = \mu F_k. \quad (5)$$

III. NUMERICAL RESULTS AND ANALYSIS OF THE GENERIC PROPAGATION OUTCOMES

A. The study of the general case when the \mathcal{PT} -symmetric linear lattice potential is different from the \mathcal{PT} -symmetric nonlinear lattice potential

In Eq. (1), we consider that the \mathcal{PT} -symmetric linear lattice profile is given by the periodic functions $v(x) = \varepsilon_0 \cos^2(x)$ and $w(x) = \omega_0 \sin(2x)$, whereas the \mathcal{PT} -symmetric nonlinear lattice modulation is given by the following periodic functions: $v_1(x) = \varepsilon_1 \cos(2x)$ and $w_1(x) = -\omega_1 \sin(2x)$, see Ref. [20], where ε_0 and ω_0 are the amplitudes of real and imaginary parts of the linear OLs, respectively, and the amplitudes ε_1 and ω_1 of the nonlinearity-modulation spatial distribution. Thus in the most general case to be studied in this subsection we take different periodic spatial distributions (different linear and nonlinear lattice potentials). Therefore for the above choice of the two jointly acting linear and nonlinear lattice potentials, the real parts, the sign of the imaginary parts, and the amplitudes of the modulation profiles are totally different.

First, we fix the parameters ε_0 and ω_0 of the \mathcal{PT} -symmetric linear lattice in order to investigate the effect of \mathcal{PT} -symmetric nonlinear lattices on soliton propagation. Solving numerically the linear eigenvalue equation (5) by using the plane wave expansion method, we obtain the corresponding band structure. We then fix the values of the two parameters describing the \mathcal{PT} -symmetric linear OLs as $\varepsilon_0 = 4$ and $\omega_0 = 0.8$. The spatial modulation profile and the corresponding band structure are displayed in Figs. 1(a) and 1(b), respectively. Then we numerically solve Eqs. (2) and (3) by the spectral renormalization

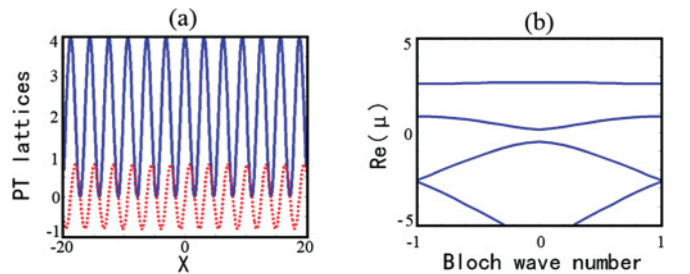


FIG. 1. (Color online) (a) \mathcal{PT} -symmetric complex-valued periodic linear OLs for $\omega_0 = 0.8$ and $\varepsilon_0 = 4$ (the solid curves represent the real part of the modulation profile, whereas the dotted curves represent the imaginary part of the modulation profile). (b) The band structure corresponding to the lattice profile shown in (a).

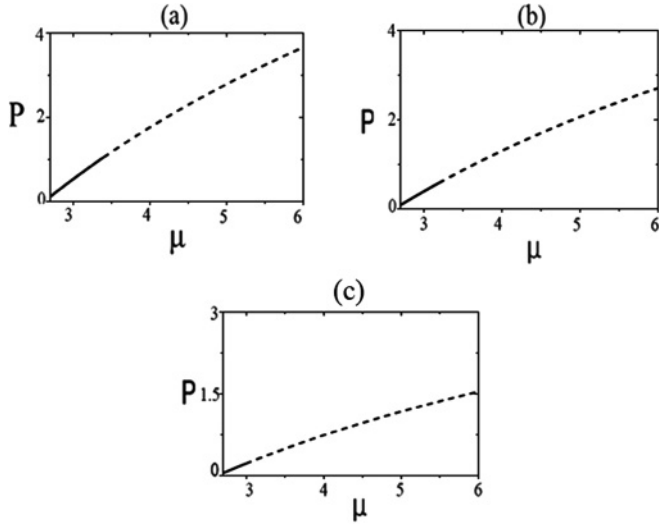


FIG. 2. Power P versus propagation constant μ for $\varepsilon_0 = 4$ and $\omega_0 = 0.8$ and (a) $\varepsilon_1 = 0.1$ and $\omega_1 = 0.1$, (b) $\varepsilon_1 = 0.5$ and $\omega_1 = 0.5$, and (c) $\varepsilon_1 = 1$ and $\omega_1 = 1$. The stable branches are plotted by solid curves and the unstable branches are plotted by dashed curves.

method [25] and the modified squared-operator method [26], respectively. The total soliton power P is defined as $P = \int_{-\infty}^{+\infty} |f|^2 dx$. The dependences of soliton power P versus propagation constant μ are shown in Figs. 2(a), 2(b), and 2(c), for three sets of nonlinear OL parameters $\varepsilon_1 = 0.1$ and $\omega_1 = 0.1$, $\varepsilon_1 = 0.5$ and $\omega_1 = 0.5$, and $\varepsilon_1 = 1$ and $\omega_1 = 1$, respectively. From Fig. 2, we see that the soliton power increases with the decrease of the amplitudes ε_1 and ω_1 of the nonlinearity-modulation spatial distribution. This can be explained as follows. Because we are considering here a self-focusing Kerr nonlinearity, if the depth of nonlinear lattice increases, the corresponding self-focusing effect exerted on the optical beam, which is determined by $[1 + v_1(x)]|q|^2 q$ and the associated nonlinear gain effect coming from the imaginary part of the nonlinear lattice potential are becoming stronger. In addition, for a certain depth of the nonlinear lattice, a higher power (or peak amplitude) of solitons will also cause a much stronger self-focusing effect on the optical beam. If the combination of self-focusing and nonlinear gain effects is stronger than a critical limit, the lattice solitons will collapse. So the existence of solitons in our specific situation requires that their peak amplitudes (or powers) must decrease with increase of the depth of the nonlinear lattice in order to avoid the destruction of the solitons during propagation due to the presence of a very high self-focusing effect. Note that if only the depth of the dissipative part of nonlinearity modulation is increased, the soliton power still decreases, i.e., the effect of the imaginary (dissipative) part of nonlinearity modulation on the soliton power is smaller than that induced by the real part of the nonlinearity modulation.

Further we investigate the longitudinal evolution of lattice solitons. The robustness of the soliton propagation is tested in direct numerical simulations of Eq. (1) by adding a random noise to the soliton (typically we add 10% of the soliton amplitude). The results of simulations are shown in Fig. 3 where we plot both the soliton field profiles and their corresponding evolutions during propagation. We get that the stable soliton regions are as follows: $2.7 \leq \mu \leq 3.4$ for $\varepsilon_1 =$

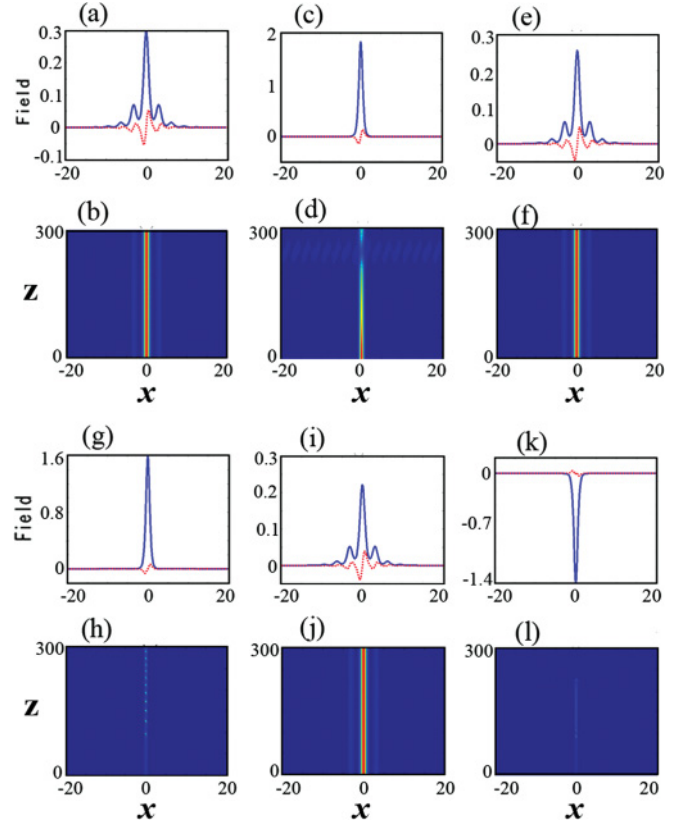


FIG. 3. (Color online) Soliton profiles (the solid curves show the real parts and the dotted curves show the corresponding imaginary parts) and soliton evolution for $\varepsilon_0 = 4$ and $\omega_0 = 0.8$. Stable soliton evolutions for $\mu = 2.7$: (a), (b) for $\varepsilon_1 = 0.1$ and $\omega_1 = 0.1$, (e), (f) for $\varepsilon_1 = 0.5$ and $\omega_1 = 0.5$, and (i), (j) for $\varepsilon_1 = 1$ and $\omega_1 = 1$. Unstable soliton evolutions for $\mu = 5$: (c), (d) for $\varepsilon_1 = 0.1$ and $\omega_1 = 0.1$, (g), (h) for $\varepsilon_1 = 0.5$ and $\omega_1 = 0.5$, and (k), (l) for $\varepsilon_1 = 1$ and $\omega_1 = 1$.

0.1 and $\omega_1 = 0.1$, $2.7 \leq \mu \leq 3.2$ for $\varepsilon_1 = 0.5$ and $\omega_1 = 0.5$, and $2.7 \leq \mu \leq 3.0$ for $\varepsilon_1 = 1$ and $\omega_1 = 1$. These results clearly show that lattice solitons can only stabilize in the low-power range and that the stable soliton domain narrows with the growth of the amplitudes ε_1 and ω_1 of nonlinear lattices. Typical stable soliton evolutions for the propagation constant $\mu = 2.7$ are plotted in Figs. 3(a), 3(b) for $\varepsilon_1 = 0.1$ and $\omega_1 = 0.1$, Figs. 3(e), 3(f) for $\varepsilon_1 = 0.5$ and $\omega_1 = 0.5$, and Figs. 3(i), 3(j) for $\varepsilon_1 = 1$ and $\omega_1 = 1$, while typical unstable soliton evolutions for $\mu = 5$ are given in Figs. 3(c), 3(d) for $\varepsilon_1 = 0.1$ and $\omega_1 = 0.1$, Figs. 3(g), 3(h) for $\varepsilon_1 = 0.5$ and $\omega_1 = 0.5$, and Figs. 3(k), 3(l) for $\varepsilon_1 = 1$ and $\omega_1 = 1$.

The lattice solitons are tightly bound by the mixed \mathcal{PT} -symmetric linear-nonlinear lattice; the high-amplitude solitons are compacted within one spatial lattice period, which is equal to π in all our simulations. The most unstable solitons experience a fast decay of energy upon propagation, whereas the less unstable ones exhibit slight oscillations of their peak amplitudes.

Next, we consider in detail the effect of varying the amplitudes of the real and imaginary parts of linear lattice potential on soliton propagation when fixing the parameters of nonlinear lattice potential; here we fix the values of the nonlinearity-modulation profile to $\varepsilon_1 = 0.5$ and $\omega_1 = 0.5$.

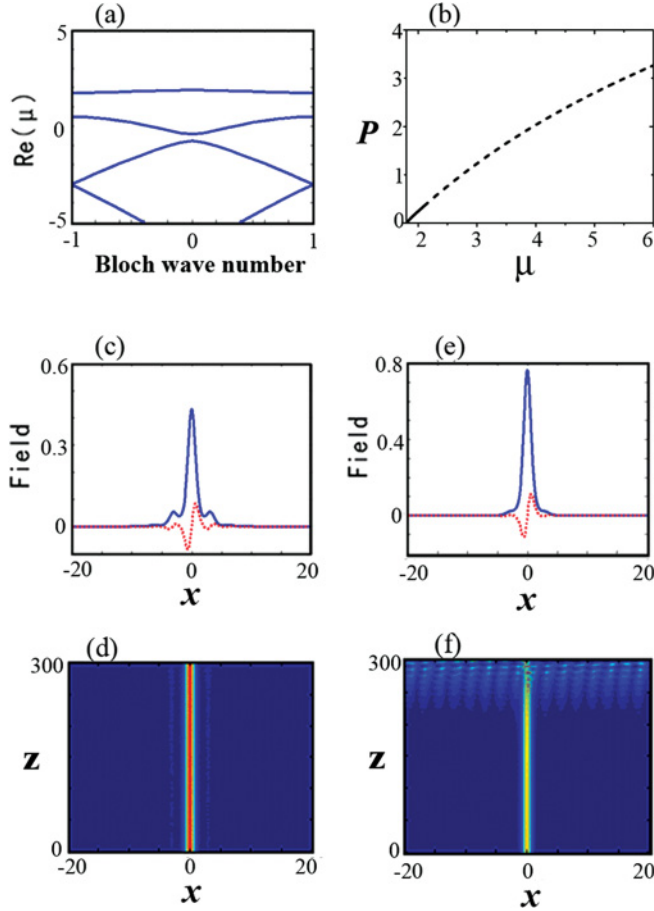


FIG. 4. (Color online) (a) The band structure and (b) total power P versus propagation constant μ for $\varepsilon_0 = 3$ and $\omega_0 = 0.8$ (the stable region is plotted by a solid curve and the unstable domain is plotted by a dashed curve). A typical stable soliton propagation for $\mu = 2.4$ (c), (d) and a typical unstable soliton propagation for $\mu = 2.4$ (e), (f). Other parameters are $\varepsilon_1 = 0.5$ and $\omega_1 = 0.5$.

On the one hand, we decrease the amplitude of the real part of linear lattice potential from $\varepsilon_0 = 4$ to $\varepsilon_0 = 3$ and we fix the second parameter of the linear lattice potential to $\omega_0 = 0.8$. The corresponding numerical results are displayed in Figs. 4(a)–4(f). These numerical simulations show that the propagation constant interval where the soliton is stable is now $1.8 \leq \mu \leq 2.1$. By comparing this result for $\varepsilon_0 = 3$ with the above-discussed case (for $\varepsilon_0 = 4$), which was shown in Fig. 2(b), we find that the stability domain is smaller and shifts towards lower values of μ . Also, it is worthy to notice that the power slightly increases if we keep constant the value of the propagation constant μ . On the other hand, if we decrease the amplitude of the imaginary part of the linear lattice potential from $\omega_0 = 0.8$ to $\omega_0 = 0.6$ we obtain the results shown in Figs. 5(a)–5(f). In this case the stability domain is $2.7 \leq \mu \leq 3.4$. By comparing this stability range with that obtained in the case when the value $\omega_0 = 0.8$ was chosen, see Fig. 2(b) [recall that the solitons were found to be stable in the interval $2.7 \leq \mu \leq 3.2$], we find that the stability region for $\omega_0 = 0.6$ is larger than that for $\omega_0 = 0.8$ and that it shifts towards higher values of the propagation constant μ . Note that the powers that correspond to the same value of the propagation

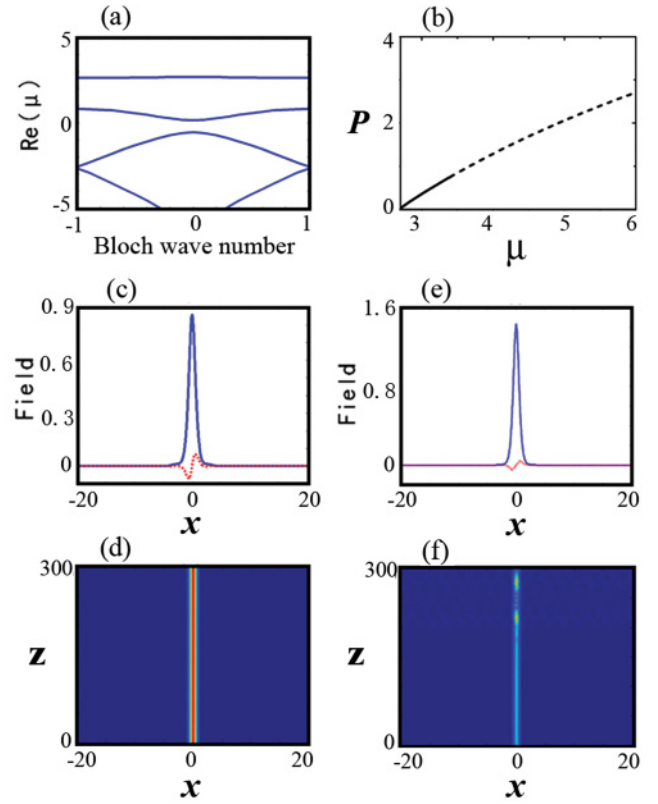


FIG. 5. (Color online) (a) The band structure for $\varepsilon_0 = 4$ and $\omega_0 = 0.6$. (b) Power P versus propagation constant μ (the stable region is plotted by the solid curve and the unstable domain is plotted by the dashed curve). A typical stable soliton evolution for $\mu = 2.9$ (c), (d) and a typical unstable soliton evolution for $\mu = 3.6$ (e), (f). Other parameters are $\varepsilon_1 = 0.5$ and $\omega_1 = 0.5$.

constant μ hardly change if the value of the parameter ω_0 of the linear lattice potential changes from $\omega_0 = 0.8$ to $\omega_0 = 0.6$.

B. The study of a special case when the \mathcal{PT} -symmetric linear lattice potential is identical with the \mathcal{PT} -symmetric nonlinear lattice potential

In what follows we investigate the special case when we consider identical \mathcal{PT} -symmetric lattice potentials for both linear and nonlinear OLs. We thus take the following modulation profiles: $v(x) = \varepsilon_0 \cos^2(x)$, $w(x) = \omega_0 \sin(2x)$, $v_1(x) = v(x)$, and $w_1(x) = w(x)$.

In order to find out the effect of modification of the amplitudes of the real and imaginary parts of the linear and nonlinear modulation profiles, on soliton propagation, we select three typical sets of parameters: (i) $\varepsilon_0 = 4$ and $\omega_0 = 0.8$, (ii) $\varepsilon_0 = 3$ and $\omega_0 = 0.8$, and (iii) $\varepsilon_0 = 4$ and $\omega_0 = 0.6$. The \mathcal{PT} -symmetric complex-valued periodic OLs and their associated band structures are displayed in Fig. 6 for $\varepsilon_0 = 4$ and $\omega_0 = 0.8$ [Figs. 6(a), 6(b)], for $\varepsilon_0 = 3$ and $\omega_0 = 0.8$ [Figs. 6(c), 6(d)], and for $\varepsilon_0 = 4$ and $\omega_0 = 0.6$ [Figs. 6(e), 6(f)]. The corresponding total powers P versus propagation constant μ are shown in Fig. 7. The stability domains are found to be $2.7 \leq \mu \leq 3.5$, $1.9 \leq \mu \leq 3.0$, and $2.7 \leq \mu \leq 4.5$, for the above sets of parameters (i), (ii), and (iii), respectively. These results clearly show that solitons can be stable only in

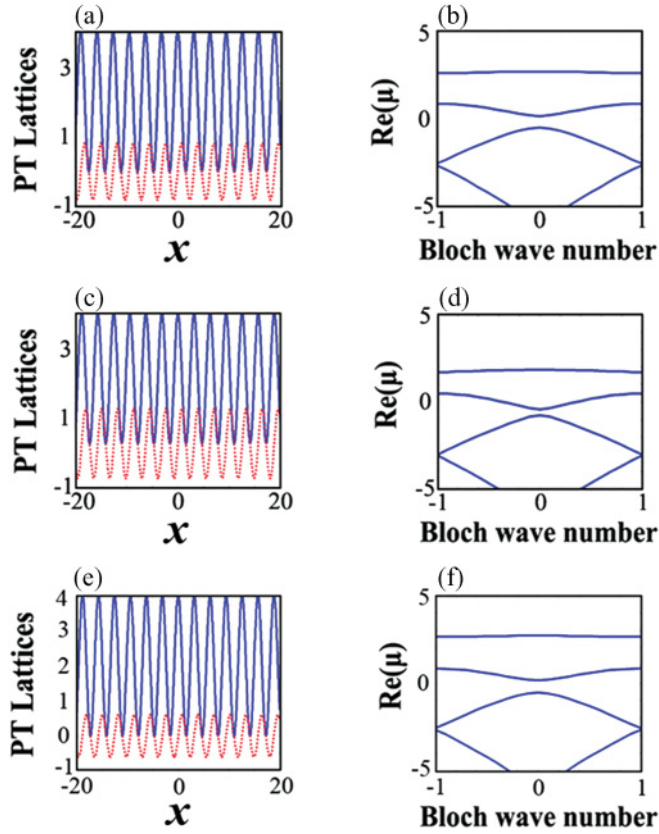


FIG. 6. (Color online) \mathcal{PT} -symmetric complex-valued periodic linear OLs for (a) $\varepsilon_0 = 4$ and $\omega_0 = 0.8$, (c) $\varepsilon_0 = 3$ and $\omega_0 = 0.8$, and (e) $\varepsilon_0 = 4$ and $\omega_0 = 0.6$. In panels (b), (d), and (f) we plot the band structures corresponding to the modulation profiles displayed in panels (a), (c), and (e), respectively.

the low-power regimes and that the soliton stability region increases with the decrease of the amplitudes of imaginary parts of modulation profiles of both kinds of OLs. Also, the

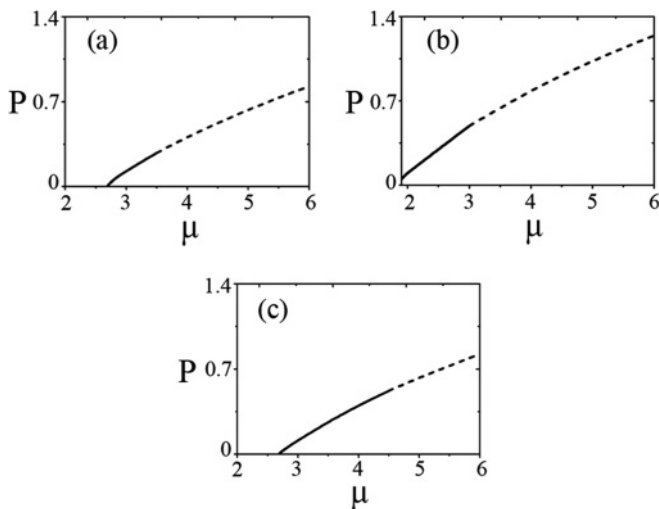


FIG. 7. Power P versus μ for (a) $\varepsilon_0 = 4$ and $\omega_0 = 0.8$, (b) $\varepsilon_0 = 3$ and $\omega_0 = 0.8$, and (c) $\varepsilon_0 = 4$ and $\omega_0 = 0.6$. The stable regions are plotted by solid curves and the unstable regions are plotted by dashed curves.

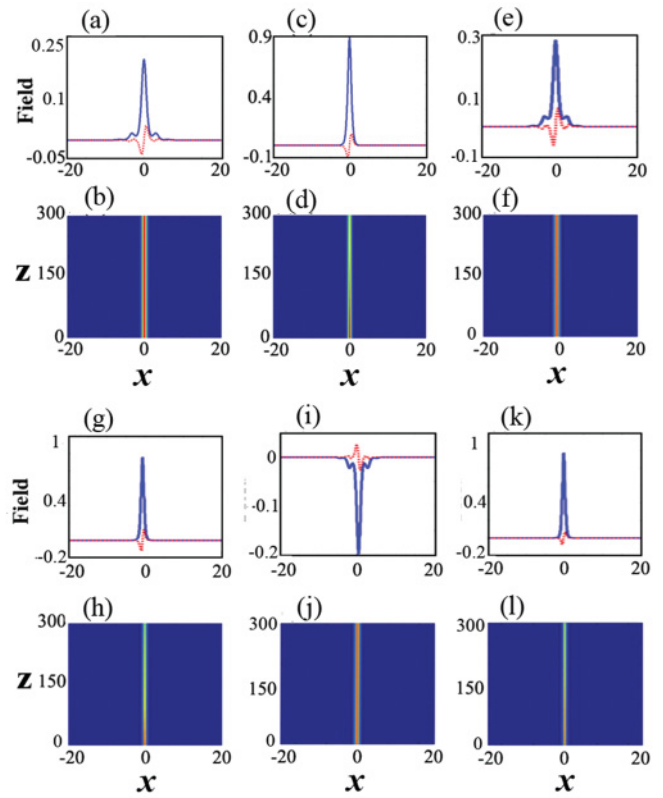


FIG. 8. (Color online) Soliton profiles and their corresponding longitudinal evolutions. Stable propagations: (a), (b) $\varepsilon_0 = 4$, $\omega_0 = 0.8$, and $\mu = 2.8$; (e), (f) $\varepsilon_0 = 3$, $\omega_0 = 0.8$, and $\mu = 2$; (i), (j) $\varepsilon_0 = 4$, $\omega_0 = 0.6$, and $\mu = 2.8$. Unstable propagations: (c), (d) $\varepsilon_0 = 4$, $\omega_0 = 0.6$, and $\mu = 5$; (g), (h) $\varepsilon_0 = 3$, $\omega_0 = 0.8$, and $\mu = 4$; (k), (l) $\varepsilon_0 = 4$, $\omega_0 = 0.8$, and $\mu = 5.5$.

soliton stability region shifts towards the lower values of μ with the decrease of the amplitude of modulation profiles of real parts of both kinds of OLs. We thus conclude that the parameters of \mathcal{PT} -symmetric linear lattices play an important role in controlling the magnitude of the soliton stability region. The soliton profiles and the longitudinal evolution of typical stable and unstable solitons are plotted in Figs. 8(a)–8(l).

Note that the present study can be extended in the direction of considering in detail the competition between linear and nonlinear lattice potentials, i.e., by choosing different gain and loss combinations of the dissipative parts of both linear and nonlinear lattice potentials.

IV. CONCLUSIONS

To summarize, in this work we reported the existence and stability domains of lattice solitons confined by the joint action of parity-time-symmetric linear and nonlinear lattices in Kerr media. We concluded that the joint action of parity-time-symmetric linear and nonlinear optical lattices can support stable propagation of solitons in the semi-infinite gap, for a variety of choices of the spatial distributions of \mathcal{PT} -symmetric periodic confining lattice potentials. The stationary soliton solutions constitute a one-parameter family in a dissipative system where the balance between gain and loss effects must be fulfilled, in contrast to zero-parameter dissipative solitons in

optical systems described by Ginzburg-Landau-like nonlinear dynamical models, see, e.g., [27,28]. Also, the comprehensive numerical calculations show that lattice solitons in such mixed linear-nonlinear lattices can stably propagate in the low-power regime, but are unstable in the higher-power one. In particular, the region of stability of soliton propagation can be controlled by tuning the values of either the real or imaginary parts of \mathcal{PT} -symmetric linear and nonlinear optical lattices. It is found that the domain where the solitons are stable can be enlarged by decreasing the imaginary parts of either linear or nonlinear lattice potentials, while the soliton stability range shifts towards lower values of μ by decreasing the real parts of linear lattice potentials. Thus the parameters of the linear lattice periodic potential play an important role in controlling the magnitude of the stability domains of lattice solitons in such mixed linear-nonlinear optical lattices.

This work may be extended to other kinds of \mathcal{PT} -symmetric nonlinear dissipative systems involving balance of gain and losses at both the linear and nonlinear level. Our results may find potential applications in controlling or routing light in optical signal processing systems.

ACKNOWLEDGMENTS

This work was supported by the National Natural Science Foundation of China (Grant No. 11174061) and the Guangdong Province Natural Science Foundation of China (Grant No. S2011010005471). The work of D.M. was supported by CNCS-UEFISCDI, Project No. PN-II-ID-PCE-2011-3-0083.

-
- [1] C. M. Bender and S. Boettcher, *Phys. Rev. Lett.* **80**, 5243 (1998).
 [2] Z. Ahmed, *Phys. Lett. A* **282**, 343 (2001).
 [3] C. M. Bender, D. C. Brody, and H. F. Jones, *Phys. Rev. Lett.* **89**, 270401 (2002).
 [4] C. M. Bender, D. C. Brody, and H. Jones, *Am. J. Phys.* **71**, 1095 (2003).
 [5] C. M. Bender, D. C. Brody, H. F. Jones, and B. K. Meister, *Phys. Rev. Lett.* **98**, 040403 (2007).
 [6] Z. H. Musslimani, K. G. Makris, R. El-Ganainy, and D. N. Christodoulides, *Phys. Rev. Lett.* **100**, 030402 (2008).
 [7] K. G. Makris, R. El-Ganainy, D. N. Christodoulides, and Z. H. Musslimani, *Phys. Rev. Lett.* **100**, 103904 (2008).
 [8] K. G. Makris, R. El-Ganainy, D. N. Christodoulides, and Z. H. Musslimani, *Phys. Rev. A* **81**, 063807 (2010).
 [9] A. Guo, G. J. Salamo, D. Duchesne, R. Morandotti, M. Volatier-Ravat, V. Aimez, G. A. Siviloglou, and D. N. Christodoulides, *Phys. Rev. Lett.* **103**, 093902 (2009).
 [10] C. E. Rüter, K. G. Makris, R. El-Ganainy, D. N. Christodoulides, M. Segev, and D. Kip, *Nat. Phys.* **6**, 192 (2010).
 [11] O. Bendix, R. Fleischmann, T. Kottos, and B. Shapiro, *Phys. Rev. Lett.* **103**, 030402 (2009).
 [12] H. Wang and J. Wang, *Opt. Express* **19**, 4030 (2011).
 [13] K. Zhou, Z. Guo, J. Wang, and S. Liu, *Opt. Lett.* **35**, 2928 (2010).
 [14] X. Zhu, H. Wang, L.-X. Zheng, H. Li, and Y.-J. He, *Opt. Lett.* **36**, 2680 (2011).
 [15] Z. Shi, X. Jiang, X. Zhu, and H. Li, *Phys. Rev. A* **84**, 053855 (2011).
 [16] S. Liu, C. Ma, Y. Zhang, and K. Lu, *Opt. Commun.* (2011), doi:10.1016/j.optcom.2011.11.065.
 [17] Y. V. Kartashov, B. A. Malomed, and L. Torner, *Rev. Mod. Phys.* **83**, 247 (2011).
 [18] S. V. Dmitriev, A. A. Sukhorukov, and Y. S. Kivshar, *Opt. Lett.* **35**, 2976 (2010).
 [19] F. Lederer, G. I. Stegeman, D. N. Christodoulides, G. Assanto, M. Segev, and Y. Silberberg, *Phys. Rep.* **463**, 1 (2008).
 [20] F. K. Abdullaev, Y. V. Kartashov, V. V. Konotop, and D. A. Zezyulin, *Phys. Rev. A* **83**, 041805 (2011).
 [21] A. E. Miroshnichenko, B. A. Malomed, and Y. S. Kivshar, *Phys. Rev. A* **84**, 012123 (2011).
 [22] S. V. Suchkov, B. A. Malomed, S. V. Dmitriev, and Y. S. Kivshar, *Phys. Rev. E* **84**, 046609 (2011).
 [23] Y. V. Bludov and V. V. Konotop, *Phys. Rev. A* **74**, 043616 (2006).
 [24] F. Abdullaev, A. Abdumalikov, and R. Galimzyanov, *Phys. Lett. A* **367**, 149 (2007).
 [25] M. J. Ablowitz and Z. H. Musslimani, *Opt. Lett.* **30**, 2140 (2005).
 [26] J. Yang and T. I. Lakoba, *Stud. Appl. Math.* **118**, 153 (2007).
 [27] *Dissipative Solitons: From Optics to Biology and Medicine*, edited by N. Akhmediev and A. Ankiewicz, Lecture Notes in Physics, Vol. 751 (Springer, Berlin, 2008); *Dissipative Solitons*, Lecture Notes in Physics, Vol. 661 (Springer, Berlin, 2005); B. A. Malomed, in *Encyclopedia of Nonlinear Science*, edited by A. Scott (Routledge, New York, 2005), p. 157.
 [28] I. S. Aranson and L. Kramer, *Rev. Mod. Phys.* **74**, 99 (2002); P. Mandel and M. Tlidi, *J. Opt. B: Quantum Semiclass. Opt.* **6**, R60 (2004); V. Skarka and N. B. Aleksić, *Phys. Rev. Lett.* **96**, 013903 (2006); D. Mihalache, D. Mazilu, F. Lederer, Y. V. Kartashov, L.-C. Crasovan, L. Torner, and B. A. Malomed, *ibid.* **97**, 073904 (2006); N. N. Rozanov, *J. Opt. Technol.* **76**, 187 (2009); J. M. Soto-Crespo, N. Akhmediev, C. Mejia-Cortes, and N. Devine, *Opt. Express* **17**, 4236 (2009); H. Leblond, B. A. Malomed, and D. Mihalache, *Phys. Rev. A* **80**, 033835 (2009); V. Skarka, N. B. Aleksić, H. Leblond, B. A. Malomed, and D. Mihalache, *Phys. Rev. Lett.* **105**, 213901 (2010); D. Mihalache, *Proc. Romanian Acad. A* **11**, 142 (2010); V. E. Lobanov, Y. V. Kartashov, V. A. Vysloukh, and L. Torner, *Opt. Lett.* **36**, 85 (2011); Y. V. Kartashov, V. V. Konotop, and V. A. Vysloukh, *ibid.* **36**, 82 (2011); D. Mihalache, *Rom. Rep. Phys.* **63**, 9 (2011); P. V. Paulau, D. Gomila, P. Colet, B. A. Malomed, and W. J. Firth, *Phys. Rev. E* **84**, 036213 (2011).